

# Preferential Wetting Phenomenon in Bicomponent Polymer Melt Flow

JOHN H. SOUTHERN, *Monsanto Company, Indian Orchard, Massachusetts 01151* and RICHARD L. BALLMAN, *Monsanto Company, Pensacola, Florida 32574*

## Synopsis

For two polymer melts spun in a side-by-side configuration through a capillary, interface shape and spinneret exit angle data are presented as a function of viscosity ratio, spinneret dimensions, and relative polymer-steel wettability. Nylon-nylon versus nylon-polyurethane bicomponent flow systems are compared. A surface tension phenomenon is postulated to be significant in controlling the bicomponent fiber interface shape for capillary length-to-diameter ratios of the order of unity.

## INTRODUCTION

Bicomponent fiber extrusion is now achieved routinely on a commercial scale, with the resulting fibers valued for their self-crimping characteristics.<sup>1-4</sup> Previous literature has demonstrated that significant interface motion occurs in side-by-side bicomponent polymer melt flow.<sup>5-7</sup> A theoretical basis has been provided for three causes of interface shape change: (i) melt viscosity,<sup>5,8,9</sup> (ii) melt elasticity,<sup>10</sup> and (iii) surface tension differences.<sup>11</sup>

For bicomponent fibers spun from polymers of similar chemical composition, the viscosity ratio was experimentally shown to be a significant variable in controlling the melt filament exit angle as it emerges from the capillary as well as the final spun filament interface shape.<sup>5,6</sup> The filament exit angle was always reported to be towards the slower-moving higher-viscosity component; and the lower viscosity component interface always curved around the higher viscosity component, producing an interfacial curvature distinctive of bicomponent fiber spinning from two unequal viscosity melts. The interface wrap-around phenomenon has been attributed to a minimum energy dissipation principle causing the higher viscosity melt to move into the lower shear rate region in the capillary center.<sup>5,8,9</sup> At equal melt viscosities, an elasticity phenomenon has also been demonstrated, with the irregular interface shape attributed to unequal second normal stress differences.<sup>6,7</sup> The research presented herein documents, for the first time, the existence of a third factor: the surface tension effect in bicomponent polymer melt spinning.

## EXPERIMENTAL

Using a laboratory bicomponent spinning machine consisting of two 1-in. extruders feeding heated channels that produce conjugate side-by-side melt flow to a spinneret and a Leesona 955 yarn take-up, polyurethane-nylon and nylon-nylon bicomponent fiber interface shapes and spinneret exit angles were com-

pared as a function of viscosity ratio and spinneret capillary geometry. The polyurethane and nylon 6 compositions are listed in Table I. Nylon sample B is always used as the common component in these studies. The interface shape is defined quantitatively as the percent extrudate periphery occupied by one component. The exit angle is the angle between the extruding fiber and a perpendicular to the spinneret face (an axis parallel with the capillary axis), as shown schematically in Figure 1. A tripod-mounted telescope equipped with a protractor scale was used to measure the exit angle fairly precisely ( $\pm 3^\circ$ ).

The nylon-polyurethane melt viscosity ratio was varied by changing the polymer melt temperature; the nylon-nylon viscosity ratio was varied by using nylons of different molecular weights. The Instron Capillary Rheometer was used to determine representative flow curves (Fig. 2) for viscosity ratio calculations. Nylon and polyurethane flow activation energies at  $10^6$  dyn/cm<sup>2</sup> shear stress, used for viscosity ratio calculations, are 15 and 50 kcal/g mole,<sup>12</sup> respectively. The parallel flow curves for the nylon and polyurethane melts examined herein resulted in a viscosity ratio essentially independent of shear rate, hence of position across the interface shape.

TABLE I  
Nylon-6 and Polyurethane Composition and  
Molecular Weights<sup>a</sup>

Nylon-6 (Polycaprolactam)			
Composition:			
	$\left[ \begin{array}{c} \text{H} \quad \text{O} \quad \quad \quad \text{O} \\   \quad \quad \quad \quad \quad \quad \quad   \\ \text{---N---C---(CH}_2\text{)}_6\text{---C---} \end{array} \right]$		
Sample	Melt viscosity (20 sec <sup>-1</sup> and 230°C; poise)	Molecular weight	
		number average, $\bar{M}_n$	weight average, $\bar{M}_w$
A	1100	11,900	29,400
B	1900	14,000	35,300
C	2700	14,450	37,700
D	3600	14,700	40,000

Polyurethane [Polyester and 4,4'-Methylenebis (Phenylisocyanate) with 1,4 Butanediol Extender]			
Composition:			
	$\left[ \begin{array}{c} \text{O} \quad \quad \quad \quad \quad \quad \quad \text{O} \\    \quad \quad \quad \quad \quad \quad \quad    \\ \text{---C---N---} \text{---} \text{CH}_2\text{---} \text{---} \text{CH}_2\text{---} \text{---} \text{N---C---O---(CH}_2\text{)}_4\text{---O---} \end{array} \right]$		
	Hard segment		
Composition:			
	$\left[ \begin{array}{c} \text{O} \quad \quad \quad \quad \quad \quad \quad \text{O} \\    \quad \quad \quad \quad \quad \quad \quad    \\ \text{---C---(CH}_2\text{)}_4\text{---C---O---(CH}_2\text{)}_4\text{---O---} \end{array} \right]$		
	Soft segment		
Melt viscosity (20 sec <sup>-1</sup> and 230°C; poise)	$\bar{M}_n$	$\bar{M}_w$	
2000	23200	66400	

<sup>a</sup> Waters GPC Model 200 with 50°C trifluoroethanol—0.05% lithium bromide solution.

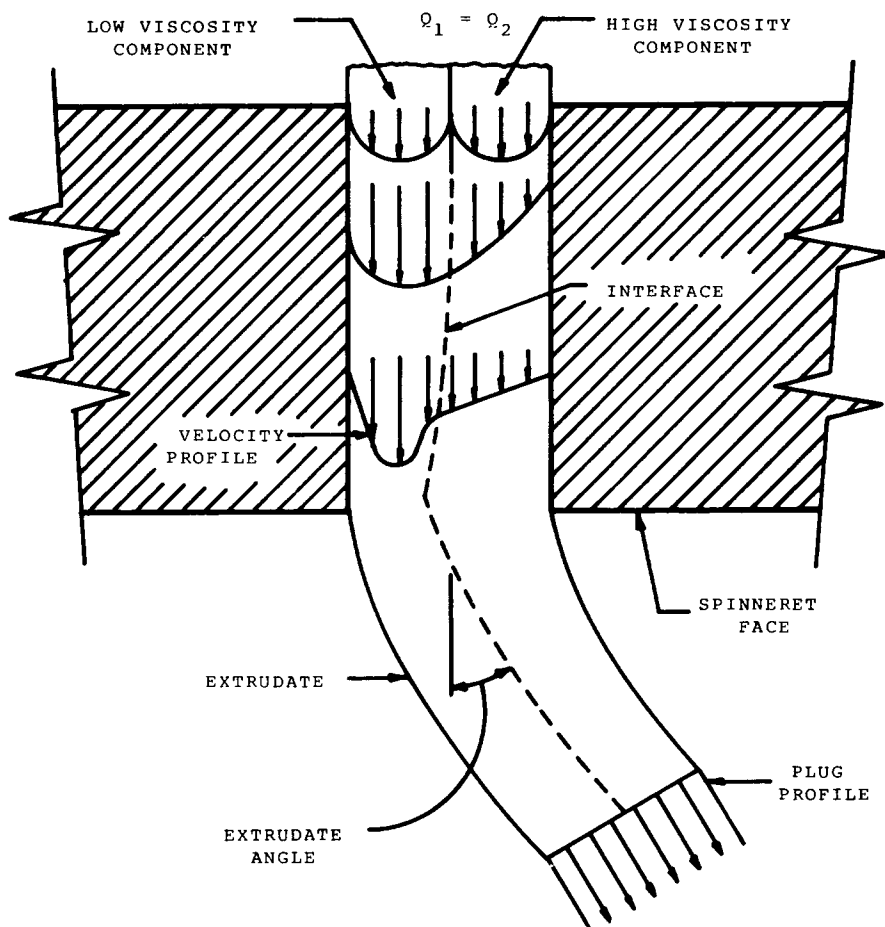


Fig. 1. Extrudate bending in bicomponent flow in parallel plates due to viscosity mismatch (equal component flow rates).

Interface shape and exit angle were also examined for two polymer-steel interfacial surface tension ratios: one for nylon-nylon and the other for a nylon-polyurethane system. To determine preferential wetting of the capillary steel wall (type 430 stainless) by polyurethane versus nylon-6, contact angles were measured from photographs of flake chips allowed to melt on a heated steel spinneret blank (see Fig. 3 schematic). A nitrogen shroud prevented polymer degradation.

Nylon and polyurethane melt elasticities have also been measured using the Rheometrics Spectrometer cone and plate. The primary normal stress coefficient values are extremely low for both nylon and polyurethane at 230°C (less than 0.01 kPa sec<sup>2</sup>) and are assumed to be negligible. N.B.: Previous research<sup>6,7</sup> has demonstrated that elasticity differences for two polymer melts in bicomponent flow can produce irregular interface shapes, but these do not resemble the changes described herein.

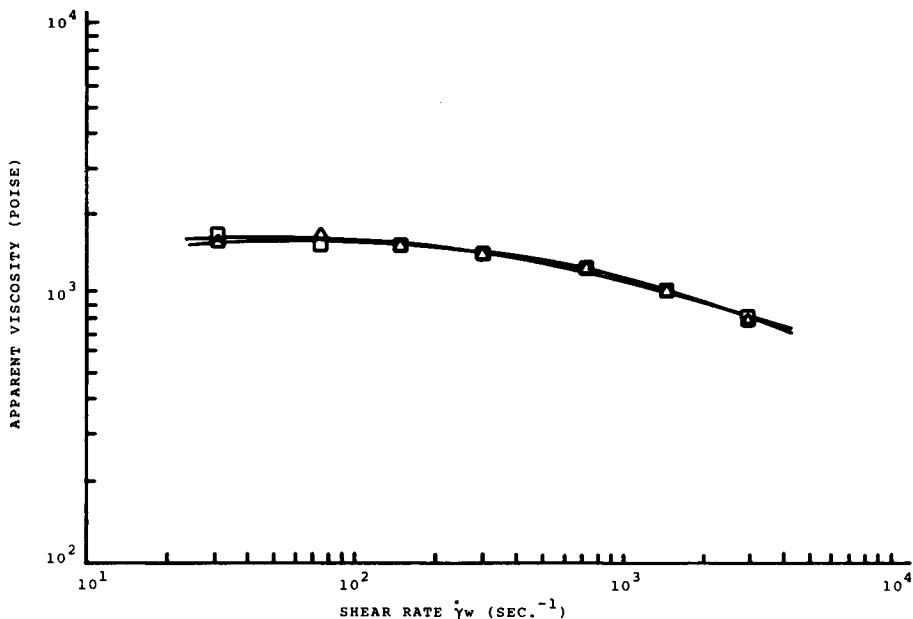


Fig. 2. Polyurethane and nylon-6 viscosity vs shear rate. ( $\square$ ) polyurethane; ( $\Delta$ ) nylon-6—sample B: Capillary = 0.050 in.  $\times$  1.99 in.  $\times$  90° entrance angle; 233.5  $\pm$  0.5°C.

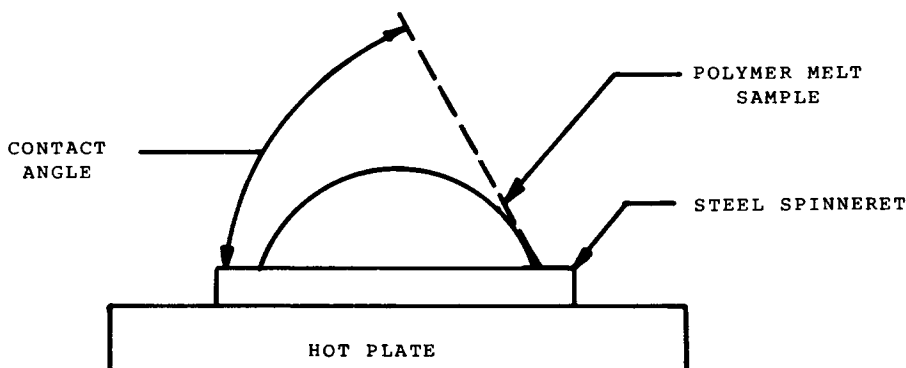


Fig. 3. Polymer-steel contact angle measurements.

## DISCUSSION

The bicomponent fiber interface shape and exit angle dependence on melt viscosity ratio is presented in Figure 4 for two nylon-6 melts of different viscosities. Consistent with previous observations on polystyrene model systems,<sup>5,6</sup> the fiber always exits from the spinneret by bending toward the high viscosity component; in addition, the interface, originally located as a diameter between the two components, always curves around the high viscosity component. Interface curvature and exit angle formation have been previously examined and attributed to the following mechanisms.<sup>5,6</sup> As the two polymer melts occupying equal areas and having equal volumetric throughput rates flow into the spinneret capillary entrance (see Fig. 1 schematic for infinite parallel plate analogy), an immediate interface movement occurs within the flow channel in order to maintain equal pressure drops keeping the equal throughputs fixed by the ex-

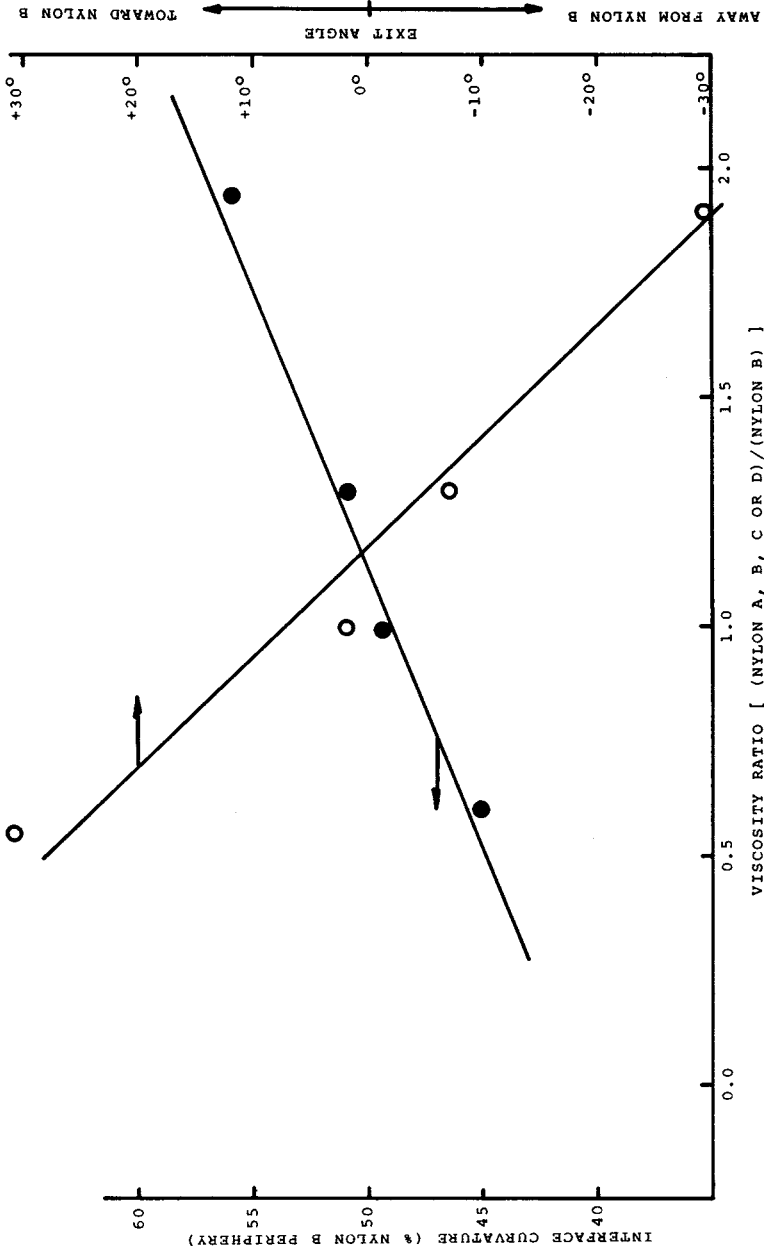


Fig. 4. Interface curvature and exit angle vs viscosity ratio for nylon-nylon bicomponent fibers. (●) Interface shapes; (○) exit angle (230°C melt; 0.025 in. diameter  $\times$  0.025 in. length capillary).

truders; the higher-viscosity, slower-moving component shifting to occupy a greater area, and portion of the channel cross section. This rapid interface movement is completely reversed on exiting from the tube, where the velocity profile becomes uniform across the solidifying fiber and equal areas are again required for equal component throughputs. This velocity profile rearrangement produces a bending moment resulting in a filament exit angle towards the slower-moving higher-viscosity component. For flow in a circular tube, the conservation of mass criterion maintaining equal throughputs at all lengths down the flow path does not lead to interface movement at the wall, where the velocity is close to zero; however, such factors as minimum energy dissipation may produce interface movement at the wall, resulting in a gradual irreversible wrap around by the lower viscosity component that produces a continuously increasing interface curvature with tube length.<sup>6</sup> As one would expect, the exit angle decreases to zero as complete wrap around occurs.<sup>9</sup>

Replotting the Figure 4 nylon-nylon data as interface curvature versus exit angle and adding comparable nylon-polyurethane bicomponent fiber data provide the Figure 5 relationships that are a function of polymer pair. The curve for the polyurethane-nylon-6 bicomponent fiber documents a barrier to nylon wrap around; i.e., the bicomponent fibers having exit angles towards the urethane component (indicating that the urethane has the higher viscosity) do not exhibit the interfacial curvature characteristic of a viscosity mismatch. Figure 6 provides data at two capillary length-to-diameter ratios, indicating that the urethane resistance to being encapsulated is only apparent for low length-to-diameter ratios. Figure 7 depicts representative urethane-nylon interface shapes as a function of viscosity ratio for the two capillaries. The longer capillary B produces the gradual interface curvature normally observed for bicomponent fibers spun from unequal viscosity melts. For the short capillary A, the urethane-nylon interface shapes at 0.8 and 1.0 viscosity ratios represent distinct anomalies. Note

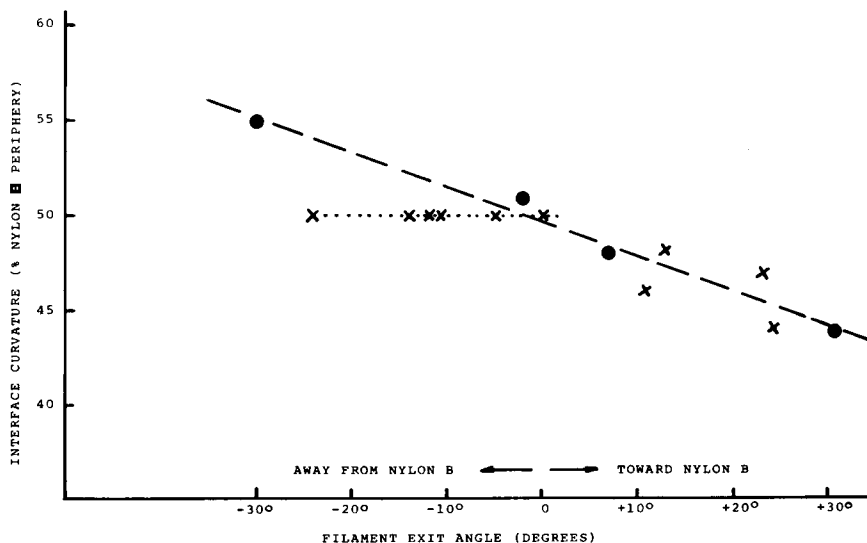


Fig. 5. Nylon-nylon and nylon-polyurethane bicomponent fiber interface curvature vs exit angle. (· · · X · · ·) nylon-polyurethane; (- - ● - -) nylon-nylon (230°C melt; 0.025 in. diameter × 0.025 in. length capillary).

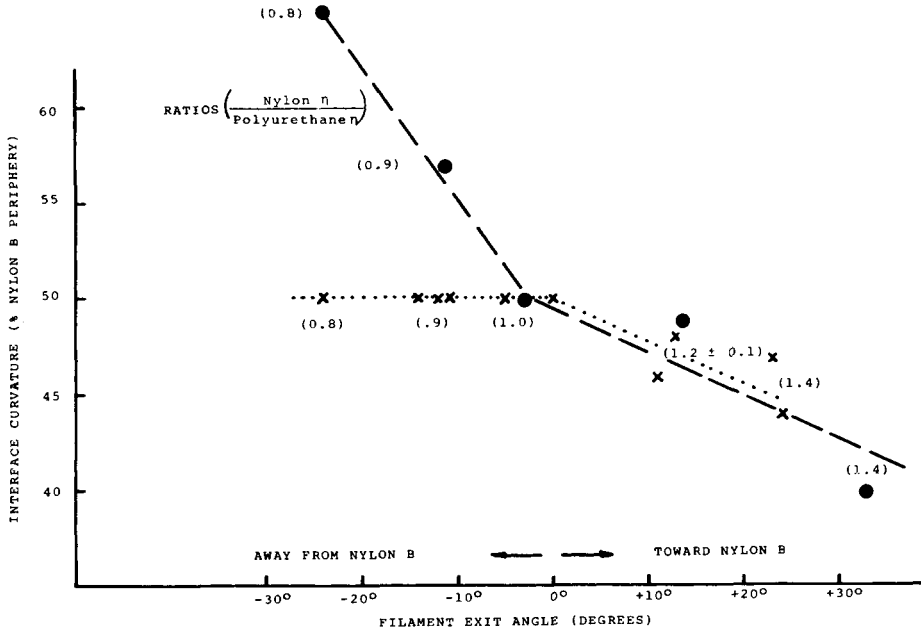
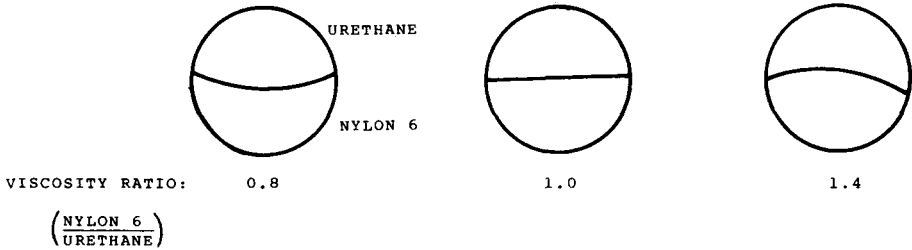


Fig. 6. Nylon-polyurethane interface curvature and exit angle as a function of capillary length-to-diameter and viscosity ( $\eta$ ). Diameter  $\times$  length: ( $\dots \times \dots$ ) 0.025 in.  $\times$  0.025 in.; ( $- \bullet - -$ ) 0.025 in.  $\times$  0.135 in.



CAPILLARY A (0.025" DIAMETER  $\times$  0.025" LENGTH)

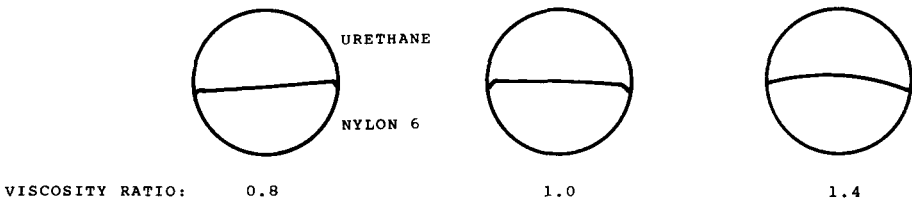


Fig. 7. Nylon-6-polyurethane interface shape vs viscosity ratio.

the sharp break in the interface near the circumference of these two fibers, where the urethane slightly wraps around the nylon in a region limited to the outer periphery. It is postulated that preferential wetting of the steel capillary wall by the urethane is the probable cause for failure of the nylon to wrap-around even though it has the lower viscosity.

Consistent with this explanation, contact angle measurements resulted in the following values for urethane and nylon on steel (see Fig. 3 schematic):

nylon-6  $71^\circ$

polyurethane  $52^\circ$

The decreased polyurethane contact angle indicates its increased ability to wet or adhere to the steel capillary wall relative to nylon. However, only for a capillary length-to-diameter ratio of the order of unity (or less) does the "wettability ratio" of the two components to the capillary surface become significant in defining the interface shape. The minimum energy dissipation driving force for interface curvature increases with capillary length-to-diameter ratio, effectively overcoming the urethane preferential wetting force at a capillary length-to-diameter ratio of 5.4 (capillary B in Fig. 7). In addition, it is of interest to note that the Figure 8 varying capillary dimension data show a linear correlation between exit angle and interface curvature for the nylon-polyurethane system, where the following spinneret geometries (at constant 5.4 length-to-diameter ratio) and flow conditions were examined:

spinneret capillary (diameter $\times$ length) (in.)	capillary wall shear rate ( $\text{sec}^{-1}$ )	average residence time in the capillary (sec)
0.015 $\times$ 0.081	5270	0.008
0.025 $\times$ 0.135	1140	0.04
0.050 $\times$ 0.270	140	0.3

The constant exit angle-interface shape correlation for this capillary diameter,

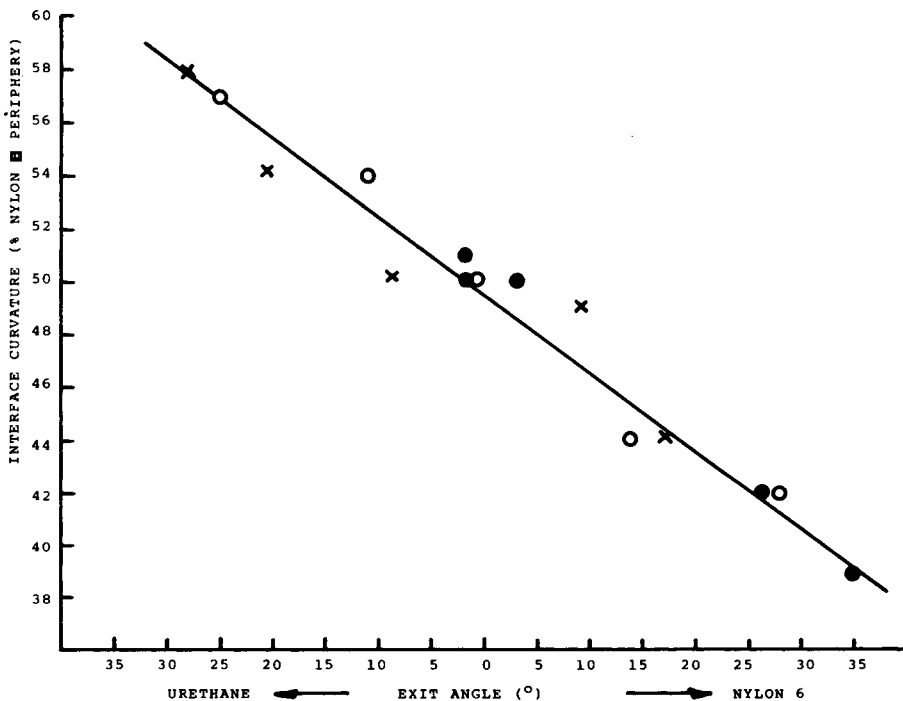


Fig. 8. Nylon-6-polyurethane interface curvature vs exit angle. Capillary diameter  $\times$  length (in.); (●) 0.015  $\times$  0.081; (○) 0.025  $\times$  0.135; (×) 0.050  $\times$  0.270.



shear rate, and residence time range suggests that the capillary length-to-diameter ratio effect exemplified in Figure 6 is the only important process variable defining the degree of irreversible interface curvature.

## CONCLUSIONS

In addition to relating bicomponent fiber interface curvature to unequal component melt viscosities<sup>5</sup> and the irregular interface shape being attributed to an elasticity mismatch,<sup>6</sup> a third factor producing interface shape change has now been demonstrated: the preferential wetting of one melt component with the capillary wall that prevents wrap around by the higher surface energy component. This surface tension phenomenon is only significant at low capillary length-to-diameter ratios of the order of unity, with the effect vanishing at higher values where the viscosity ratio effectively controls the interface shape observed. This research completes a series of three bicomponent flow studies in which individual effects of polymer melt viscosity, elasticity, and surface tension ratios were examined. Clearly, the viscosity ratio dominates bicomponent flow with surface tension and elasticity ratios producing minor changes in the interface shape under very limited bicomponent flow conditions.

The assistance provided by D. H. Martin and D. A. Kehoe in defining laboratory spinning conditions is gratefully acknowledged, as is the Instron Rheometer and bicomponent fiber interface curvature data provided by E. W. Craddock and J. A. Burroughs. The excellent spinneret designs of L. M. Moore were essential to the spinneret geometry evaluation. The support and helpful suggestions of J. H. Saunders and K. R. Lea provided the stimulus necessary for successful completion of this research.

## References

1. J. H. Saunders, J. A. Burroughs, L. P. Williams, D. H. Martin, J. H. Southern, R. L. Ballman, and K. R. Lea, *J. Appl. Polym. Sci.*, **19**, 1387 (1975).
2. E. M. Hicks, J. F. Ryan, R. B. Taylor, and R. L. Techinor, *Text. Res. J.*, **30**, 675 (1960).
3. R. A. Buckley and R. J. Phillips, *Chem. Eng. Prog.*, **66**, 41 (1969).
4. A. E. Shiekh, J. F. Bogdan, and R. K. Gupta, *Text. Res. J.*, **41**, 281 (1971).
5. J. H. Southern and R. L. Ballman, *Appl. Polym. Symp.*, **20**, 175 (1973); originally published in *Am. Chem. Soc. Polym. Prepr.*, **13**, 106 (1972).
6. J. H. Southern and R. L. Ballman, *J. Polym. Sci. Polym. Phys. Ed.*, **13**, 863 (1975).
7. C. D. Han, *J. Appl. Polym. Sci.*, **17**, 1289 (1973).
8. A. E. Everage, Jr., *Trans. Soc. Rheol.*, **17**, 629 (1973).
9. A. E. Everage, Jr., *Trans. Soc. Rheol.*, **19**, 509 (1975).
10. J. L. White, R. C. Ufford, K. R. Dharod, and R. L. Price, *J. Appl. Polym. Sci.*, **16**, 1313 (1972).
11. D. Hasson, U. Mann, and A. Nir, *Can. J. Chem. Eng.*, **48**, 514 (1970).
12. J. H. Southern, R. L. Ballman, and J. H. Saunders, *J. Appl. Polym. Sci.*, submitted for publication.

Received November 13, 1978

Revised January 3, 1979